

Estimates of Confusion and Gravitational Lensing Limits in Sunyaev–Zel’dovich Increment Measurements

Michael Zemcov¹, Peter Newbury¹, Mark Halpern¹

¹ *Department of Physics & Astronomy, University of British Columbia, Vancouver, BC, Canada*

Draft 2003 February 22

ABSTRACT

We present estimates of the confusion limit of measurements of the Sunyaev–Zel’dovich effect (SZ) increment near its peak intensity based on Monte Carlo simulations of sub-millimetre observations of galaxy clusters. Specifically, we evaluate the contribution of gravitational lensing of high redshift background sources by a target cluster to its inferred SZ signal. We find that the background confusion limit is 0.6 mJy per beam without any lensing. With gravitational lensing, the confusion limit increases to 0.9 mJy per beam. Removing bright sources in the gravitationally lensed fields decreases the confusion limit to 0.7 mJy per beam, essentially background levels. These limits are found by removing exceptionally poor fits to the expected SZ profile, which are due to the different structure of the SZ and lensing angular profiles.

We conclude that experiments designed to measure the SZ increment must have high enough angular resolution to identify background point sources while surveying enough of the sky to determine the SZ profile. Observations of the SZ increment with SCUBA, which has sufficient sensitivity and resolution for the task, should be straight forward.

Key words: galaxies: clusters: general – cosmic microwave background – cosmology: gravitational lensing – methods: numerical – methods: statistical

1 INTRODUCTION

The Sunyaev–Zel’dovich (SZ) effect is a spectral distortion of the cosmic microwave background (CMB) radiation. It is caused by the interaction of CMB photons and highly energetic electrons in a plasma. Usually, this plasma is the diffuse $T_e = 10^7$ K gas present near the center of a galaxy cluster. On average, CMB photons are scattered to shorter wavelengths in collisions with relativistic electrons, producing a decrement in apparent CMB temperature at long wavelengths and an increment at short wavelengths. Measurements of the SZ increment, particularly at its 850 μ m peak, will be a very important probe of the Universe’s large scale structure in the future (e.g. Birkinshaw (1999)). However, many diverse effects conspire to make measurement of the sub-millimetre (sub-mm) SZ increment difficult, including the brightness of the sub-mm sky, the need for stable, accurate instrumentation, and the small amplitude of the SZ increment signal.

SZ increment measurements are made more challenging still because of other sources of flux in a cluster field. These miscellaneous flux sources include the Butcher–Oemler effect, the Rees–Sciama effect, and gravitational lensing of primordial CMB anisotropies. Blain (1998) gives a detailed discussion of these sources of flux in galaxy clusters, and comes to the conclusion that none of these effects produces

a signal strong enough to compete with the SZ increment in galaxy clusters.

However, source confusion can play a large part in increasing the danger of erroneous measurements. The term source confusion is used to describe the variance in flux observed in a map due to unresolved, faint sources in the field, the level of which depends on the resolution of the telescope and the background source number count in the observational passband. While it is true that sub-mm emission from within an X-ray cluster is rare, background sources at higher redshift, z , are common and relatively bright. This means that source confusion is inevitable in a cluster field, and may mimic the SZ effect. The effect of source confusion may be compounded many times by gravitational lensing, which brightens high z background sources behind a cluster. This paper evaluates the effect of gravitational lensing and its contribution to source confusion in sub-mm measurements of the SZ effect.

We are engaged in a program to measure the SZ increment in X-ray bright clusters with the Sub-millimetre Common User Bolometer Array (SCUBA) on the James Clerk Maxwell Telescope (JCMT). We wish to determine the confusion limit of these measurements so that we can design a statistically valid observing program, and additionally to determine if gravitational lensing of background sources by the target cluster will worsen the confusion limit or bias

our estimate of the size of the effect. A preliminary description of the measurements themselves is found in Zemcov et al. (2002), hereafter Paper I. We have performed Monte Carlo simulations of SCUBA observations of galaxy clusters including lensing and a realistic source model. Blain (1998) has studied this problem previously, but was forced to model galaxy formation and evolution using optical and infrared source counts since observationally determined sub-mm background source counts were not available. Further, Blain (1998) considers only single pixel measurements of the SZ effect while we use the high resolution available with SCUBA to identify point sources and remove them from analysis. A standard ($\Omega_M = 0.3, \Omega_\Lambda = 0.7$) cosmology is assumed (Bennett et al. (2003)), and all errors are $1\text{-}\sigma$ unless otherwise stated.

2 EXPERIMENT

2.1 Lensed Sub-mm Map Simulations

In order to realistically simulate the effect of gravitational lensing on source confusion, accurate source counts are required. Borys et al. (2002) have analyzed sub-mm HDF data and conclude that the number of sources with amplitudes greater than flux S , $N(> S)$, is

$$N(> S) = N_0 \left(\frac{S}{S_0} \right)^{-\alpha} \left(1 + \frac{S}{S_0} \right)^{-\beta} \quad (1)$$

with $S_0 = 10$ mJy, $\alpha = 0.8$, $\beta = 2.5$, and $N_0 = 1.55 \times 10^3$ deg $^{-2}$. We assume that the SCUBA background sources are at most weakly clustered on scales relevant to this experiment. This means that a Poisson distribution of sources uniformly and randomly distributed in a field is fully consistent with the data.

Because equation (1) yields cumulative counts, we take its numerical derivative. For each amplitude bin, a Poisson distribution with mean equal to the number of sources in that bin is used to give a random number of sources for each amplitude bin consistent with the source counts. A random number from a uniform distribution ranging between the limits of the relevant amplitude bin is added to each of the source amplitudes to randomize the source strengths. This procedure produces an ensemble of random source strengths in the range 0.01 mJy to 25 mJy. Each point source amplitude is then associated with a uniformly distributed random position in the field. The simulated map created in this way is referred to as a ‘background’ field and is statistically the same as a sub-mm field observed at random in the sky. Because SCUBA sources are all likely to be background objects, they will all be lensed to some extent when observed in the region of a foreground cluster.

Our gravitational lensing algorithm is based on that used in Newbury & Spiteri (2002)¹, and the parameteric lensing model utilized in this experiment is the singular isothermal sphere (SIS). If \mathbf{y} is the position of the point source in the source plane in arcsec, \mathbf{x} is the position of the lensed image in the deflector plane in arcsec, D_{ds} is the

distance between the source and the deflector, D_s is the distance to the source, and σ is the velocity dispersion of the deflector in km s $^{-1}$, then the lensing model is

$$\mathbf{y} = \mathbf{x} - 28.8 \frac{D_{ds}}{D_s} \left(\frac{\sigma}{1000} \right)^2 \frac{\mathbf{x}}{|\mathbf{x}|}. \quad (2)$$

The numerical values 28.8 and 1000 have the units arcsec and km s $^{-1}$ respectively. Note that because the SIS model is spherically symmetric, changes in the apparent position of the sources must be radial. The distances are comoving distances determined via integration over redshift using the standard cosmology mentioned in the Introduction. The values of the parameters z_d and σ are chosen to be the experimentally determined values for Cl 0016 + 16 (see Table 1), as it is one of the clusters studied in Paper I. Although a relatively simple model, the SIS quite accurately parametrizes gravitational lensing by spherical mass distributions.

The distance parameters in equation (2) are computed using $z_s = 2.5$ in our simulations. We can assume all sources are in a plane at one redshift because the z dependence of the lens equation and the effect of cosmological dimming approximately cancel above $z \simeq 1$, effectively producing a 2 dimensional lensing background. The redshifts of the background SCUBA sources are not known, and so an estimate for \bar{z} must be made. It is thought that they reside in the range $1 < z < 4$, with a peak number density between $z = 2$ and $z = 3$. Because the increase due to gravitational lensing is approximately constant above $z \simeq 1$ and the sources’ redshifts are not known, simulations using a constant source redshift of 2.5 are the same as those using a redshift of 3.5 or 4.5.

Table 1: Cl 0016 + 16 Parameters

Parameter	Value	Reference
z_d	0.55	Reese et al. (2000)
σ	1324 km s $^{-1}$	Smail et al. (1995)

As well as shifting an image’s location, lensing amplifies the flux of the background sources. The SIS is used to analytically determine radial change and amplification as a function of initial position for each source in the background field; the map produced in this way is referred to as a ‘lensed’ map.

To simulate the telescope’s response to a group of point sources properly, the lensed map is convolved with a Gaussian beam with the same FWHM as the JCMT. If desired, an SZ effect signal can be inserted into the map at this point. Additionally, point sources greater than a given flux limit may be removed from the field at this stage. This map is referred to as a ‘convolved’ field, or as a ‘convolved and cleaned’ field.

2.2 SZ Effect Amplitude Determination

SCUBA measurements are differenced in order to minimize the effects of emission from the atmosphere and the telescope itself. In order to properly simulate a differential instrument’s response to the sky, it is necessary for simulated maps to be sampled in the same way as the sky is in an actual measurement. Real SCUBA pointing data (taken from a 3 hour integration in Paper I) is played across the convolved field. Random noise equal to that of a real observation is

¹ A general realization of this algorithm can be found at <http://www.astro.ubc.ca/people/newbury/siam/lens.html>. Here we have used a version restricted to circular lenses.

added to the time stream; data from bolometers made noisy by this process are removed from subsequent analysis.

A matrix inversion method is used to produce a seven pixel ‘map’ of the data (this method is discussed in Wright, Hinshaw & Bennett (1996)). In this map, the i th pixel gives the average value of the map in an annulus with outer radius $40i$ arcsec and inner radius $40(i-1)$ arcsec. This binning can be applied to SZ data as the SZ effect intensity distribution is spherically symmetric to first order. A singular value decomposition (SVD) method is used to invert the matrix (Press et al. (1992)). An example of data points determined via this method is shown in Fig. 1.

Commonly, an isothermal β model, given by equation (3), is used to describe SZ effect intensity distributions. If I is the SZ increment flux at angular distance θ from the centre of the cluster, I_0 is the central increment value, and θ_c and β are parameters characterizing the cluster, then

$$I = I_0 \left(1 + \frac{\theta^2}{\theta_c^2} \right)^{(1-3\beta)/2}. \quad (3)$$

In our simulations, the characteristic values are taken to be $\theta_c = 50$ arcsec and $\beta = 0.75$. These are representative of values one finds in observations of clusters (e.g. Reese et al. (2000)). A flux density, I_0 , which corresponds to the flux of a point source in the central bolometer is recorded. A generalized χ^2 must be used to characterize the goodness of fit, as the data points determined via SVD are heavily correlated. If x_m are the model points, x_d are the data points, and C_{ij} is the correlation matrix found in the SVD, then

$$\chi^2 = (x_m - x_d)_i C_{ij}^{-1} (x_m - x_d)_j. \quad (4)$$

The isothermal β profile is fit to the data points and the amplitude I_0 and χ^2 of the fit is recorded. The amplitude information allows us to understand the source confusion we expect, while the χ^2 statistic is a gauge of how well the isothermal β profile describes our data. A good fit is characterized by a χ^2 approximately equal to the number of degrees of freedom in our fit, namely 5. An example of an isothermal β profile fit to simulated data is shown in Fig. 1. Because the data set consists of differences, it is insensitive to the mean brightness. Fitting an isothermal β profile is therefore a two parameter fit for the baseline and amplitude.

2.3 Confusion Limit Determination

This simulation process is repeated N times to build a statistical understanding of the source confusion we expect in a typical observation of a cluster. Fig. 2A shows the best fit SZ amplitude and χ^2 for $N = 100$ simulations of observations of unlensed background fields.

Fig. 2B shows the inferred SZ amplitudes obtained in $N = 400$ simulations of observations of gravitationally lensed fields produced as described above. From these figures, it can be observed that gravitationally lensed cluster fields often yield larger SZ fits than unlensed fields do. However, a very large χ^2 accompanies a gravitationally lensed field’s larger amplitude, vastly increasing the likelihood that the fit would be rejected. This is because the lensed source appears at the Einstein ring, not at the cluster centre.

Fig. 2C shows $N = 100$ simulations of observations of

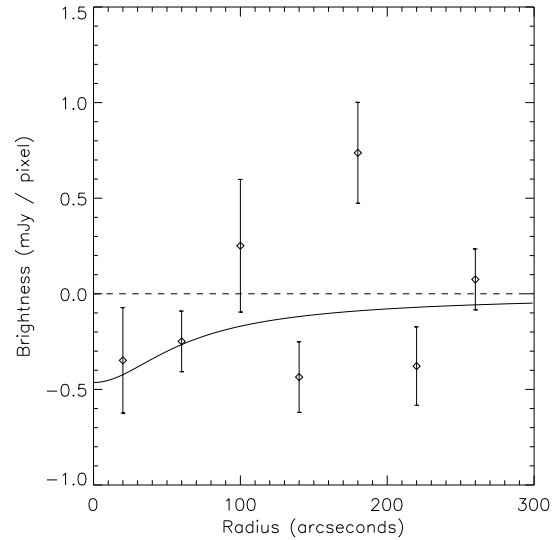


Figure 1. The results of a typical simulation described in Section 2.2. The points are averages over annular rings with 40 arcsec widths found via a matrix inversion method. The solid line below the dashed zero level is the best fit isothermal β profile given in equation (3). The fit happens to be negative in this simulation, but in general can have either sign.

gravitationally lensed fields with sources greater than 6 mJy removed. This is approximately the $3\text{-}\sigma$ level for one night’s observing. In order to avoid biasing our analysis scheme, we remove sources greater than 6 mJy in the target beam, and greater than 12 mJy in the off-source beam. In the SCUBA double difference there is one target position and two off-source positions in any given observation, with the array integrating on each off-source position for half as long as it does on the target position. Thus, a point source in either of the off-source positions will be reported as having negative one half its amplitude in the reconstructed image. This means that a negative 6 mJy point source in a map actually has a positive 12 mJy amplitude on the sky, and could have originated in *either* off-source field of view. Notice that removing the $3\text{-}\sigma$ detections essentially removes all the high χ^2 fits from the population.

Fig. 3 shows histograms of the I_0 from Figure 2 in the three cases. The standard deviations of the distributions shown in the three panels of Fig. 3 are $\sigma_A = 0.63$ mJy per beam, $\sigma_B = 36.9$ mJy per beam and $\sigma_C = 1.54$ mJy per beam. These do not characterize the widths of these non-Gaussian distributions well. We choose to define the confusion limit to be the standard deviation of these distributions after excluding those fits for which $\chi^2 \geq 20$. This χ^2 cut removes 9% and 11% of distributions A and C. We calculate χ^2 based on the detector noise, whereas the variance due to confusion is 2.3 times larger than detector noise. Therefore, we expect this cut to remove 10% of the sources in these two nearly Gaussian distributions. However, 140 of the 400 simulations in panel B are removed by the χ^2 cut since that distribution has a large tail of positive detections. The resulting confusion limits are 0.58 mJy per beam for unlensed fields, 0.85 mJy per beam for lensed clusters with poor χ^2 samples removed, and 0.66 mJy per beam for lensed clusters with $3\text{-}\sigma$ sources removed. The means of the three

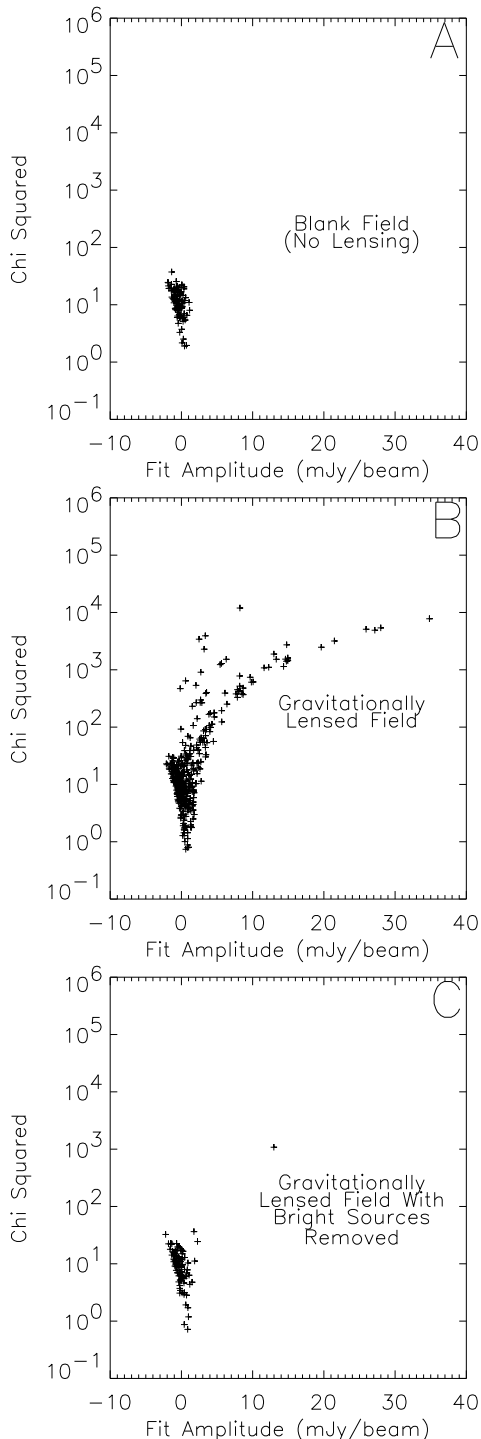


Figure 2. The results of our confusion limit simulations. Each of these plots shows χ^2 as a function of isothermal β profile amplitude for N simulations. Panel A is the data from $N = 100$ simulations of background fields. Panel B shows the data for $N = 400$ simulations of gravitationally lensed fields with no bright sources removed. The high value of N is necessary to give a good sampling as the distribution is sparse in the gravitationally lensed case. Panel C shows the data from $N = 100$ simulations of gravitationally lensed fields with point sources greater than 6 mJy in the ‘on source’ beam and greater than 12 mJy in the ‘chopped’ beam removed. These plots show that gravitational lensing and the SZ effect have different radial profiles, and fits where large lensed objects are present in the field are poorly described by the data.

distributions in Fig. 3, after the χ^2 cut, are all consistent with zero.

Although not presented as a plot here, it should be noted that including an SZ increment of amplitude I_0 mJy per beam in these simulations does change their character. The distributions in the three panels of Figure 2 are all simply displaced from zero by I_0 mJy per beam.

3 DISCUSSION AND CONCLUSIONS

Our simulations show that the SZ effect confusion limit of SCUBA observations of gravitationally lensed background fields is greater than that of unlensed fields if no attempt is made to assess quality of fit or to recognize and remove point sources.

The distributions in Fig. 3 can be compared to the results in Condon (1974) for different values of his parameter γ , which parametrizes the brightness of the population of point sources causing the bulk of the confusion in a data set. The blank field distribution shown in Fig. 3A is well described by a Gaussian distribution ($\gamma \rightarrow 3^-$) which shows that unlensed confusion is dominated by dim sources. Fig. 3B shows the distribution from gravitationally lensed fields; the confusion is dominated by bright sources ($\gamma \rightarrow 2^+$). However, when bright sources are removed from the gravitationally lensed fields as in Fig. 3C, the confusion limit is reduced to near background levels. This implies that removing bright point sources allows for a robust measurement of the SZ increment in galaxy clusters.

Our simulations show that sub-mm sources with fluxes greater than 15 mJy occur in approximately half of all gravitationally lensed fields. This matches the count rate of bright sources in sub-mm observations of galaxy clusters well: about 50 per cent of clusters observed in sub-mm surveys contain source brighter than 15 mJy (e.g. Smail et al. (2000); Cowie, Barger & Kneib (2002)). For comparison, of three clusters we have observed with SCUBA, one contains an approximately 40 mJy gravitationally lensed arc (Scott et al. (2002)), and two do not contain sources substantially greater than 10 mJy.

We find that it is possible to detect the SZ increment robustly with an instrument having sufficient angular resolution that bright sources can be recognized. This is because large amplitude gravitationally lensed background sources produce a signal recognizably different from the SZ profile.

The confusion limit of cluster fields, once lensed sources have been removed, is 0.7 mJy per beam, limiting the signal to noise ratio per cluster for the thermal effect to be under ten. A large number of clusters must be examined in order to obtain a statistically valid survey of cluster peculiar velocities. The alternative of observing only in excellent weather so that SCUBA’s short wavelength channel can aid in identifying confusion sources has not been examined.

We recommend observing a cluster until the $3\text{-}\sigma$ limit for point source detection is ~ 6 mJy. At this point detector noise will be a completely inconsequential part of determining the SZ amplitude; confusion noise will dominate. Not surprisingly, if point source confusion and lensing were not an issue one could detect the SZ increment in much less time.

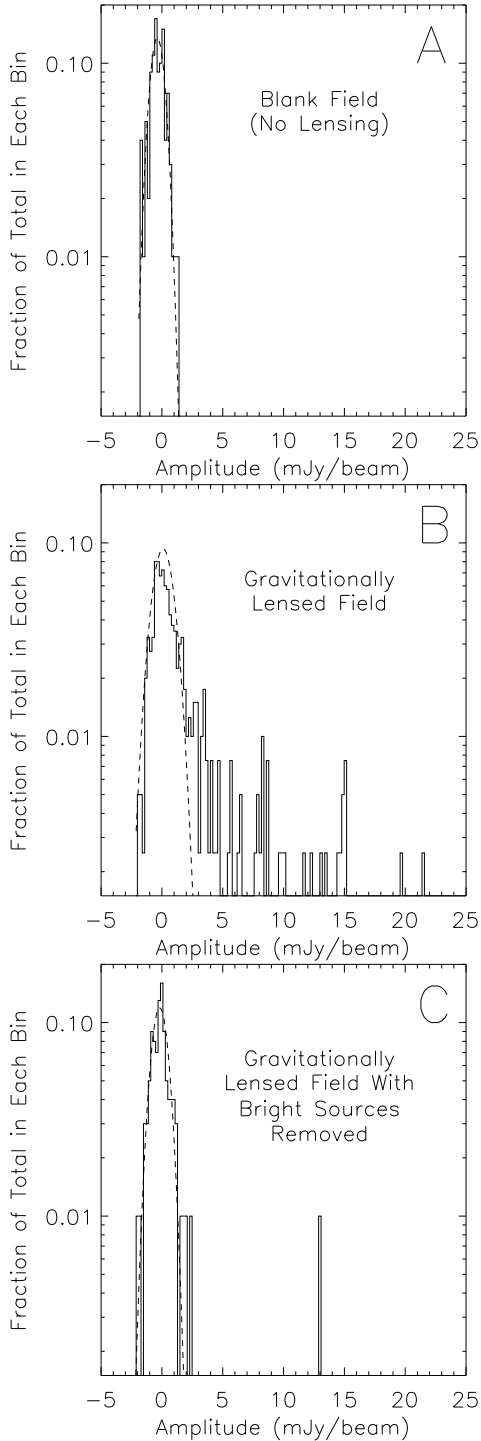


Figure 3. Histograms of the amplitudes in the data sets shown in Figure 2 (no χ^2 cut has been applied). Gaussian distributions with mean and variance equal to the final confusion limits quoted in the text are shown as dashed lines. Panel A shows isothermal β profile fit peak amplitudes for blank sky. Panel B is the same for gravitationally lensed fields. Panel C shows amplitudes for gravitationally lensed fields with sources greater than 6 mJy removed. These show that while source confusion in gravitationally lensed fields is dominated by bright sources, confusion in both the blank sky and bright sources removed cases are dominated by dim sources.

ACKNOWLEDGMENTS

Many thanks to Douglas Scott for his helpful suggestions. This work was supported by the Natural Sciences and Engineering Research Council of Canada.

REFERENCES

- Bennett C. L., et al., 2003, ApJ, In Press
 Birkinshaw M., 1999, PhysRep, 310, 97
 Blain A. W., 1998, MNRAS, 297, 502
 Borys C., Chapman S. C., Halpern M., Scott D., 2002, MNRAS, 330, L63
 Condon J. J., 1974, ApJ, 188, 279
 Cowie L. L., Barger A. J., Kneib J. P., 2002, AJ, 123, 2197
 Newbury P. R., Spiteri R. J., 2002, SIAM Review, 44, 111
 Press W. H., Teukolsky S. A., Vetterling W. T., Flannery B. P., 1992, Numerical Recipes in C (2nd Ed.). Cambridge Univ. Press, Cambridge, UK
 Reese E. D., et al., 2000, ApJ, 533, 38
 Scott D., Borys C., Chapman S. C., Donahue M., Fahlman G. G., Halpern M., Newbury, P., 2002, AAS Meeting, 201, 128.01
 Smail I., Ellis R. S., Fitchett M. J., Edge A. C., 1995, MNRAS, 273, 277
 Smail I., Ivison R. J., Owen F. N., Blain A. W., Kneib J. P., 2000, ApJ, 528, 612
 Wright E. L., Hinshaw G., Bennett C. L. 1996, ApJL, 458, L53
 Zemcov M., Halpern M., Scott D., Borys C., Chapman S., Holland W., 2002, AAS Meeting, 201, 5.01

This paper has been produced using the Royal Astronomical Society/Blackwell Science \LaTeX style file.